INSTITUTE OF PHYSICS PUBLISHING JOURNAL OF PHYSICS B: ATOMIC, MOLECULAR AND OPTICAL PHYSICS

J. Phys. B: At. Mol. Opt. Phys. **34** (2001) 2057–2069 www.iop.org/Journals/jb PII: S0953-4075(01)22567-X

Coherent phase control in electron scattering by hydrogen atoms in a bichromatic laser field

Aurelia Cionga[1], **Fritz Ehlotzky**[2,3] **and Gabriela Zloh**[1]

[1] Institute for Space Science, PO Box MG-23, R-76900 Bucharest, Romania
[2] Institute for Theoretical Physics, University of Innsbruck, Technikerstrasse 25, A-6020 Innsbruck, Austria

E-mail: Fritz.Ehlotzky@uibk.ac.at

Received 6 March 2000, in final form 2 April 2001

Abstract

We consider electron scattering by hydrogen atoms in a bichromatic linearly polarized laser field of frequencies ω and 3ω and we discuss the coherent control of the scattering process as a function of the relative phase φ between the two components of the radiation field. The electrons are assumed to have sufficiently high energies in order to permit the description of the scattering process in the first-order Born approximation. The scattered electrons, embedded in the bichromatic laser field of moderate power, as well as the laser dressing of the hydrogen atoms in their ground state are described by time-dependent perturbation theory. We discuss the angular dependence of the nonlinear differential scattering cross sections for the low values $N = \pm 2$ of absorbed or emitted laser photons as a function of the relative phase φ between the two radiation field components. We also compare our results with those obtained from the assumption of a static potential describing the target atom.

(Some figures in this article are in colour only in the electronic version; see `www.iop.org`)

1. Introduction

About 10 years ago it was suggested in a seminal work by Shapiro *et al* [1] that it should be possible to manipulate molecular reactions by using a bichromatic laser field of frequencies ω and 2ω or ω and 3ω and by varying the relative phase of the two components of the radiation field. This method was termed by these authors as 'coherent phase control'. A considerable number of papers on this method and its applications have now been published and we refer to the reviews by Shapiro and Brumer and by one of the present authors for more details [2,3]. A few years ago, one of us applied this method to the investigation of electron–atom scattering in a bichromatic laser field [4–6], describing the atomic target by a structureless potential, as was done in the original work by Bunkin and Fedorov [7] and by Kroll and Watson [8] for a monochromatic radiation field. The same problem was also reconsidered by Milošević [9]

[3] Author to whom correspondence should be addressed.

0953-4075/01/102057+13$30.00 © 2001 IOP Publishing Ltd Printed in the UK

and by Rabadán *et al* [10]. Representing the target atom by a potential is a permissible approximation as long as the frequency of the laser field is sufficiently low, as was shown quite a number of years ago by Lami and Rahman [11, 12]. Hence, electron–hydrogen scattering in a bichromatic field was investigated [13], taking into account the effect of the laser interaction with the atomic electron in the first order of time-dependent perturbation theory, using, however, the closure approximation in order to facilitate the summation over the intermediate electron states. The same problem was treated by Ghalim and Mastour [14] for helium in a more adequate way. Using time-dependent perturbation theory to describe the colliding electron–atom system in the laser field, the importance of the laser dressing of the target system was also considered in the monochromatic case by Dubois *et al* [15] and by Kracke *et al* [16], whereas in the bichromatic case of frequencies ω and 2ω this problem was treated by two of the present authors [17, 18], in particular for higher frequencies of the laser field. In general, in this paper we shall call the influence on, and the coupling of the atomic states by the laser field 'dressing effects'. For moderate laser field intensities, for which the amplitude $\mathcal{E}$ of the laser field strength is much smaller than the Coulomb field strength $\mathcal{E}_c$ on the first Bohr orbit, these dressing effects can be treated by time-dependent perturbation theory.

In this paper we want to study two-photon free–free transitions in electron–hydrogen scattering if the radiation field is a superposition of two components of frequencies ω and 3ω. The vector potential in the dipole approximation will be given by

$$\vec{\mathcal{A}}(t) = \vec{\varepsilon}\mathcal{A}_0 \cos\omega t + \vec{\varepsilon}'\mathcal{A}'_0 \cos(3\omega t + \varphi). \tag{1}$$

$\mathcal{A}_0$ and $\mathcal{A}'_0$ are the amplitudes of the vector potentials describing the radiation fields of frequencies ω and $\omega' = 3\omega$, respectively, while $\vec{\varepsilon}$ and $\vec{\varepsilon}'$ are the associated polarization vectors. φ is the relative phase between the harmonic and the fundamental field and we shall perform a systematic study of its influence on the laser-assisted signals corresponding to scattered electrons of the final energy

$$E_f = E_i \pm 2\omega \tag{2}$$

where $E_{i(f)}$ is the initial (final) energy of the scattered particle. In the presence of the radiation field (1), the energies (2) can be reached by two different quantum paths. In figure 1 we show schematically the paths for the case $E_f > E_i$. In this figure, two identical photons of frequency ω are absorbed in the process labelled by (a), the electron gains energy 2ω since the internal state of the atom is not affected by the scattering. In the other path (b), a harmonic photon 3ω is absorbed and a fundamental photon ω is emitted. Both paths lead to the same final energy $E_f = E_i + 2\omega$. The relative phase φ in (1) 'modulates' the quantum interference between the two paths. This modulation is discussed in detail below.

For high electron energies and low radiation field intensities, we can treat our problem by means of perturbation theory. By this approximation we mean that we treat the electric field in second-order time-dependent perturbation theory and take into account the scattering potential in the first order of the Born approximation in order to evaluate the differential cross sections of the scattered electrons. We shall describe the corresponding calculations in section 2. They will be performed by taking into account all the Feynman diagrams which are involved in each of the two paths (a) and (b). This procedure turns out to be an adequate treatment of two-photon free–free transitions, including the modification of the target by the radiation fields in second-order perturbation theory. Our problem comprises the quantum interference of two processes involving the same number of photons, namely $N = \pm 2$, yielding the energy spectrum of the scattered electrons in the second pair of sidebands. It represents the simplest case in which 'coherent phase control' can be investigated, taking consistently into account the radiation dressing of the target. Although our problem involves two second-order processes,

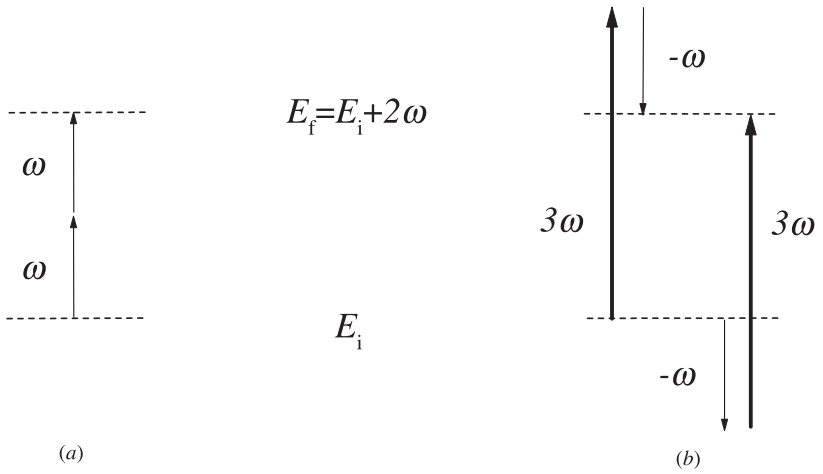

Figure 1. Energy diagrams representing schematically two-photon free–free transitions between the initial state, in which the scattered particle has energy E_i, and the final state, where it has energy $E_f = E_i + 2\omega$: (*a*) refers to the absorption of two photons of frequency ω; (*b*) corresponds to the absorption of a harmonic photon 3ω and the emission of a laser photon ω. The laser photons are represented by thin lines and the harmonic photons by thick lines.

it is more suitable for discussing interference and phase effects than the consideration of the first pair of sidebands ($N = \pm 1$), since here the interference would involve one- and three-photon processes. Our numerical examples, to be presented in section 3, were obtained for identical linear polarizations, $\vec{\varepsilon} = \vec{\varepsilon}'$, of the two field components. In the scattering geometry considered, the polarization vector $\vec{\varepsilon}$ was taken parallel to the initial momentum $\vec{p}_i$ of the ingoing electron. We used fast electrons of initial energy $E_i = 100$ eV, and took three different fundamental radiation frequencies, namely $\omega = 1.17$ eV of a Nd:YAG laser, $\omega = 3$ and 4 eV. The higher frequencies were chosen to demonstrate the increasing importance of the laser dressing of the target atom. The phase effects were analysed for small scattering angles in the case of $\omega = 1.17$ eV, where the influence of target dressing on the coherent control of the cross sections is expected to be appreciable, while for the higher radiation frequencies the scattering process was also investigated numerically for larger scattering angles. A summary of our results and some concluding remarks will be presented in section 4. Atomic units will be used throughout this work.

2. Derivation of the basic equations

The time evolution of the electron–hydrogen system in the presence of the electromagnetic field (1) is determined by the Hamiltonian

$$\mathcal{H} = \frac{\vec{P}^2}{2} - \frac{1}{R} + \frac{\vec{p}^{\,2}}{2} + \frac{1}{|\vec{r} - \vec{R}|} - \frac{1}{r} + \frac{1}{c}\left[\vec{p} + \vec{P}\right] \cdot \vec{\mathcal{A}}(t) \equiv H_0 + V + W(t) \tag{3}$$

where $\vec{R}$ and $\vec{P}$ are the position and momentum operator, respectively, of the atomic electron and $\vec{r}$ and $\vec{p}$ are the corresponding operators of the scattered electron. $V \equiv -r^{-1} + |\vec{r} - \vec{R}|^{-1}$ describes the e–H interaction in the direct channel. Exchange effects can be neglected at the higher scattering energy considered. $W(t) \equiv c^{-1}\left[\vec{p} + \vec{P}\right] \cdot \vec{\mathcal{A}}(t)$ describes the interaction of the charged particles with the radiation field in the velocity gauge, using the dipole approximation. The $\vec{\mathcal{A}}^2$-term was eliminated by a unitary transformation.

In the first non-vanishing order of perturbation theory, the S-matrix element of the two-photon process is given by

$$S^{(2)} = -\int_{-\infty}^{+\infty} \mathrm{d}t_1 \int_{-\infty}^{t_1} \mathrm{d}t_2 \, \langle \chi_f^- | \widetilde{W}(t_1) \widetilde{W}(t_2) | \chi_i^+ \rangle \tag{4}$$

with $\widetilde{W}(t) = \mathrm{e}^{\mathrm{i}H_0 t} W(t) \, \mathrm{e}^{-\mathrm{i}H_0 t}$. In the foregoing equation, $|\chi_i^+\rangle$ and $|\chi_f^-\rangle$ describe, respectively, the initial and final state of the colliding electron–atom system

$$|\chi_i^+\rangle = |\Psi_i\rangle + G^+(E_i) V |\Psi_i\rangle \tag{5}$$

$$|\chi_f^-\rangle = |\Psi_f\rangle + G^-(E_f) V |\Psi_f\rangle \tag{6}$$

where

$$G^{\pm}(E) = [E - H_0 - V \pm \mathrm{i}\delta]^{-1} \tag{7}$$

with δ a positive infinitesimal number. $|\Psi_{i,f}\rangle$ represent the asymptotic states of the colliding system in the absence of the interaction potential V and are given by

$$|\Psi_i\rangle = |\psi_{1\mathrm{s}}\rangle |K_i\rangle \tag{8}$$

$$|\Psi_f\rangle = |\psi_{1\mathrm{s}}\rangle |K_f\rangle. \tag{9}$$

$|\psi_{1\mathrm{s}}\rangle$ denotes the ground-state wavefunction of the hydrogen atom and $|K_{i,f}\rangle$ are plane waves for the ingoing and scattered electron. The initial and final energy of the electron–atom system is given by

$$E_i = E_{1\mathrm{s}} + \frac{p_i^2}{2} \qquad E_f = E_{1\mathrm{s}} + \frac{p_f^2}{2} \tag{10}$$

where $E_{1\mathrm{s}}$ is the unperturbed ground-state energy of the hydrogen atom and $p_{i(f)}$ is the initial (final) momentum of the scattered electron.

We want to study the two-photon process leading to the same final energy of the scattered electron, given by (2). This process is described by the following transition matrix element, following from (4):

$$\begin{aligned} T_{fi}^{(\pm 2)} = \frac{1}{4} \mathcal{A}_0^2 \langle \chi_f^- | \vec{\varepsilon} \cdot (\vec{p} + \vec{P}) \; G^+(\mathcal{E}_i \pm \omega) \; \vec{\varepsilon} \cdot (\vec{p} + \vec{P}) | \chi_i^+ \rangle \\ + \mathrm{e}^{\mp \mathrm{i}\varphi} \, \frac{\mathcal{A}_0 \mathcal{A}_0'}{4} [\langle \chi_f^- | \vec{\varepsilon} \cdot (\vec{p} + \vec{P}) \; G^+(\mathcal{E}_i \pm 3\omega) \; \vec{\varepsilon}' \cdot (\vec{p} + \vec{P}) | \chi_i^+ \rangle \\ + \langle \chi_f^- | \vec{\varepsilon}' \cdot (\vec{p} + \vec{P}) \; G^+(\mathcal{E}_i \mp \omega) \; \vec{\varepsilon} \cdot (\vec{p} + \vec{P}) | \chi_i^+ \rangle]. \end{aligned} \tag{11}$$

The upper sign refers to the process in which the energy of the scattered electron is increased by 2ω and the lower sign belongs to the case in which the energy is decreased by 2ω. For the sake of simplicity, we discuss here the significance of the two terms in (11) for the case $E_f > E_i$ only, as shown in figure 1, since the other case $E_f < E_i$ can be treated in a similar way. The first term in (11), which is proportional to the intensity of the fundamental field, represents the transition matrix element for the process in which two *identical* photons are absorbed and we denote this term by T_a. The second term is evidently proportional to the interference of both components of the field (1) and is connected with the diagrams in figure 1(*b*). It involves two *different* photons: a harmonic photon 2ω is absorbed and a laser photon ω is emitted. We denote this term by T_b. We point out that any higher-order correction to these leading terms are at least of the fourth order in the radiation field. In order to describe our two scattering processes for $N = \pm 2$, we only need to match the two individual matrix elements T_a and T_b by the appropriate exponential factor containing the *relative phase* φ. We infer from (11)

$$T_{fi}^{(\pm 2)} = T_a + \mathrm{e}^{\mp \mathrm{i}\varphi} T_b. \tag{12}$$

The detailed evaluation of individual matrix elements, T_a and T_b, was extensively discussed in the cited literature. For their analytic treatment the 'two-potential' formalism was used by Kracke *et al* [16] in the case of two identical photons and by Cionga and Buică [17] for the present problem of two different photons. In these investigations, the above-mentioned authors considered high scattering energies such that the first-order Born approximation can be employed to treat the electron–atom scattering problem. In that case, the transition matrix element can be evaluated in the third order of perturbation theory, namely in the second order of the electric field and in the first order of the scattering potential V, as noted before. If all the Feynman diagrams involved are considered, every transition matrix element for a two-photon process can be written as a sum of three terms. For example, the process shown in figure 1(a) is described by

$$T_a = T_E^a + T_M^a + T_A^a \tag{13}$$

and a similar term can be written down for the process of figure 1(b). The terms $T_E^{a(b)}$, $T_M^{a(b)}$ and $T_A^{a(b)}$ account for the electronic, mixed and atomic contributions, respectively. Each contribution is associated with a specific Feynman diagram, as was discussed in [16, 17]. The angular behaviour of these three contributions, as well as their dependence on the frequencies and on the momentum transfer, was analysed in these papers. We should mention that the analytic expressions for T_a and T_b are the same for $\Delta E_\pm = E_f - E_i = \pm 2\omega$. However, for the two different signs of $\Delta E_\pm$ these expressions have to be evaluated for different values of the arguments of the Green function in (11). The same holds true for T_b.

The differential cross sections for the scattered electrons with the final energies (2) are then given by

$$\frac{\mathrm{d}\sigma(\pm 2)}{\mathrm{d}\Omega} = (2\pi)^4 \frac{p_f}{p_i} |T_{fi}^{(\pm 2)}|^2 \tag{14}$$

where

$$|T_{fi}^{(\pm 2)}|^2 = |T_a|^2 + |T_b|^2 + 2\,\mathrm{Re}\left(T_a^* T_b \mathrm{e}^{\mp \mathrm{i}\varphi}\right). \tag{15}$$

The third term in the previous expression (15) describes the *coherent interference effects* that depend on the phase difference φ between the two field components. For bichromatic fields whose frequencies satisfy the relation $3\omega < |E_{1s}|$, the two matrix elements T_a and T_b can be shown to be real. In that case, the phase dependence becomes much simpler and we find from (14) and (15)

$$\frac{1}{I^2}\frac{\mathrm{d}\sigma(\pm 2)}{\mathrm{d}\Omega} = (2\pi)^4 \frac{p_f}{p_i}\left[\mathcal{T}_a^2 + \frac{I'}{I}\mathcal{T}_b^2 + 2\sqrt{\frac{I'}{I}}\mathcal{T}_a\mathcal{T}_b\cos\varphi\right]. \tag{16}$$

In this relation we explicitly displayed the intensity dependence of the different terms of the differential cross section formula, introducing the following notation: $T_a = I\,\mathcal{T}_a$ and $T_b = \sqrt{II'}\,\mathcal{T}_b$. In these relations, I denotes the intensity of the fundamental laser field and I' that of the harmonic field. Since in the perturbative regime the power law is valid for the intensity dependence, we have normalized our results with respect to the square of the intensity of the fundamental radiation field. Therefore, in the perturbative regime the normalized differential cross sections become independent of the laser intensity and depend only on the ratio of the intensities of the two field components. As we can infer from (16), the φ dependence of the differential cross sections of our problem is symmetric with respect to $\varphi = \pi$.

3. Numerical examples and discussion

In order to investigate the coherent phase effects in two-photon free–free transitions, we carried out numerical calculations of the differential cross sections (16) for fast electrons of initial energy $E_i = 100$ eV and for three different optical frequencies. We show our results for the frequency of a Nd:YAG laser $\omega = 1.17$ eV and for the higher frequencies $\omega = 3$ eV and $\omega = 4$ eV where we expect larger dressing effects for the target atom by the bichromatic field. Both components of the field (1) have linear polarization in the same direction along the momentum $\vec{p}_i$ of the ingoing electron, namely $\vec{\varepsilon} = \vec{\varepsilon}' \equiv \vec{p}_i/p_i$, and $\vec{\varepsilon}$ defines our z-axis. In the case of the lowest frequency, we studied the phase effects at small scattering angles, where the dressing of the target atom is expected to be important so that all three terms (electronic, mixed and atomic) in (13) will contribute [16, 17]. For the higher frequencies we also considered larger scattering angles where laser dressing of the target atom can still be recognized. For the numerical evaluation of the individual transition matrix elements T_a and T_b we used the analytic expressions, involving a series of hypergeometric functions, derived previously [17, 19].

In figures 2(a) and (b) we show three-dimensional plots. The differential cross sections (16) are presented as a function of the scattering angle θ and of the relative phase φ for equal intensities $I = I'$ of the two field components. (a) refers to $\Delta E_+ = 2\omega$ and (b) to $\Delta E_- = -2\omega$. In order to understand the variation of the data shown on these surfaces, we point out that the general structure of the differential cross section (16) is given by

$$\frac{1}{I^2}\frac{\mathrm{d}\sigma(\pm 2)}{\mathrm{d}\Omega} \sim \mathcal{L}(\theta) + \mathcal{L}'(\theta)\cos\varphi \tag{17}$$

where

$$\mathcal{L}(\theta) = \mathcal{T}_a^2 + \frac{I'}{I}\mathcal{T}_b^2 \qquad \mathcal{L}'(\theta) = 2\sqrt{\frac{I'}{I}}\mathcal{T}_a\mathcal{T}_b \tag{18}$$

with $\mathcal{L}(\theta) \geqslant 0$. From the θ dependence of the individual matrix elements, T_a and T_b, follows the dependence on the scattering angle of the two quantities $\mathcal{L}$ and $\mathcal{L}'$. Moreover, these quantities depend on the momentum transfer of the scattered particle and on the field frequencies ω and 3ω. The two deep minima, appearing in the data of figures 2(a) and (b) for the same relative phase $\varphi = 180^\circ$, occur because $\mathcal{L} \simeq \mathcal{L}'$ for $\theta \simeq 11^\circ$, if $\Delta E_+ = 2\omega$, and for $\theta \simeq 6^\circ$, if $\Delta E_- = -2\omega$. The 'surface' in figure 2(b) for two-photon emission is simpler because the kinematical minimum, located at $\theta = \arccos(p_i/p_f)$, is missing in this case since $p_f < p_i$. This was discussed by Kracke *et al* [16].

Further information is revealed in figure 3, in which we display the differential cross sections $I^{-2}\,\mathrm{d}\sigma(+2)/\mathrm{d}\Omega$ as a function of the relative phase φ for six particular values of the scattering angle in the region where the laser dressing is important. The parameters are the same as in figure 2(a). For a given scattering angle and for $\varphi \neq 0$, the laser-assisted signals are increased or decreased depending on the sign of $\mathcal{L}'$ in (17). For all of those values of θ for which one of the transition matrix elements T_a or T_b vanishes due to a dynamical interference between the three terms in (13), the laser-assisted signals become φ-independent. For example, this is the case at $\theta \simeq 13.4^\circ$ where $T_b = 0$. The first three changes of the curvature of the presented data, shown in (a) and (b), (c) and (d), and (e) and (f) have their origin in the three zeros of the first matrix element T_a. They are located at $\theta \simeq 4.4^\circ, 6.4^\circ$ and 10.25°, respectively. In general, the φ dependence changes its curvature after the occurrence of a zero of the individual matrix elements, T_a and T_b, that is due to a cancellation between the electronic, mixed and atomic contributions in (13). There are only two changes of curvature encountered in figure 2(b) since

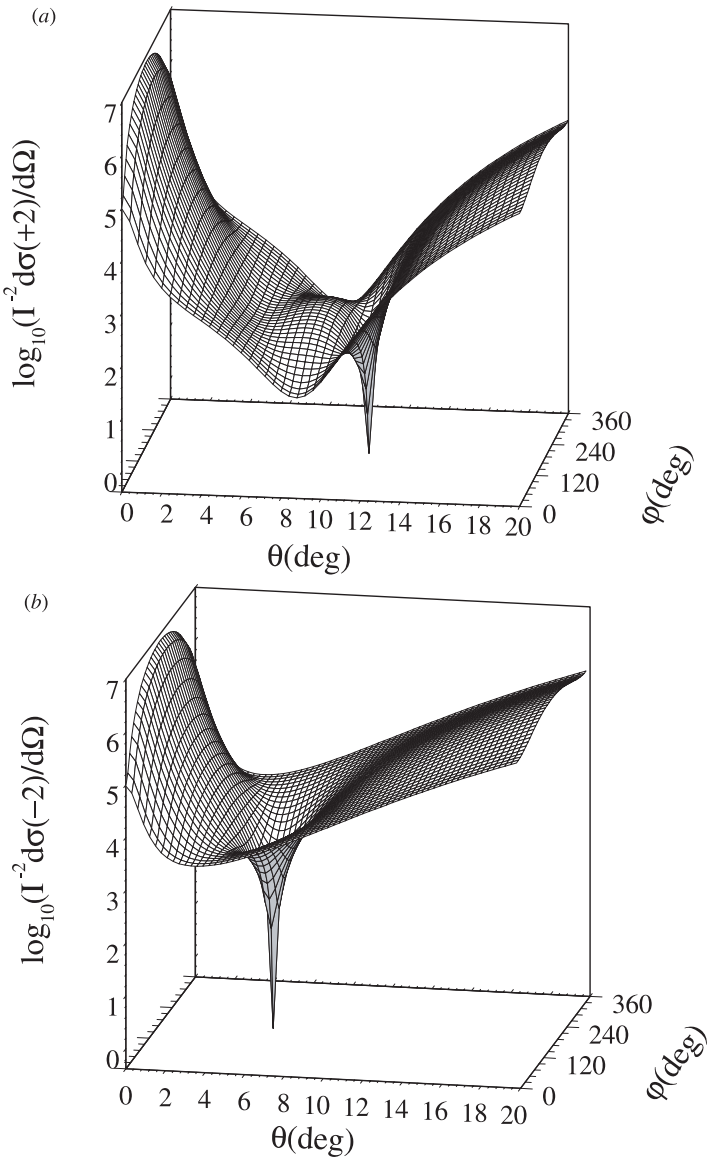

Figure 2. Part (*a*) shows on a logarithmic scale $I^{-2}\,\mathrm{d}\sigma(+2)/\mathrm{d}\Omega$, evaluated from (16), as a function of the scattering angle θ and the relative phase φ. The initial energy is $E_i = 100$ eV and the laser frequency is $\omega = 1.17$ eV. The intensity of the harmonic field was chosen to be equal to that of the laser radiation. In (*b*) we present the same as in (*a*) but for $I^{-2}\,\mathrm{d}\sigma(-2)/\mathrm{d}\Omega$.

only two such cancellations take place if $\Delta E_- = -2\omega$, namely one for T_a and another one for T_b.

The features discussed in the previous paragraph are the signature of the dressing of the target. If this dressing is neglected, the shape of the curves describing the φ dependence does not depend on the scattering angle θ, as is apparent from the dotted curves in figure 3. These curves represent $I^{-2}\,\mathrm{d}\sigma(+2)/\mathrm{d}\Omega$ computed from the approximation in which only the first term in equation (13) for T_a is retained and, similarly, in the equivalent

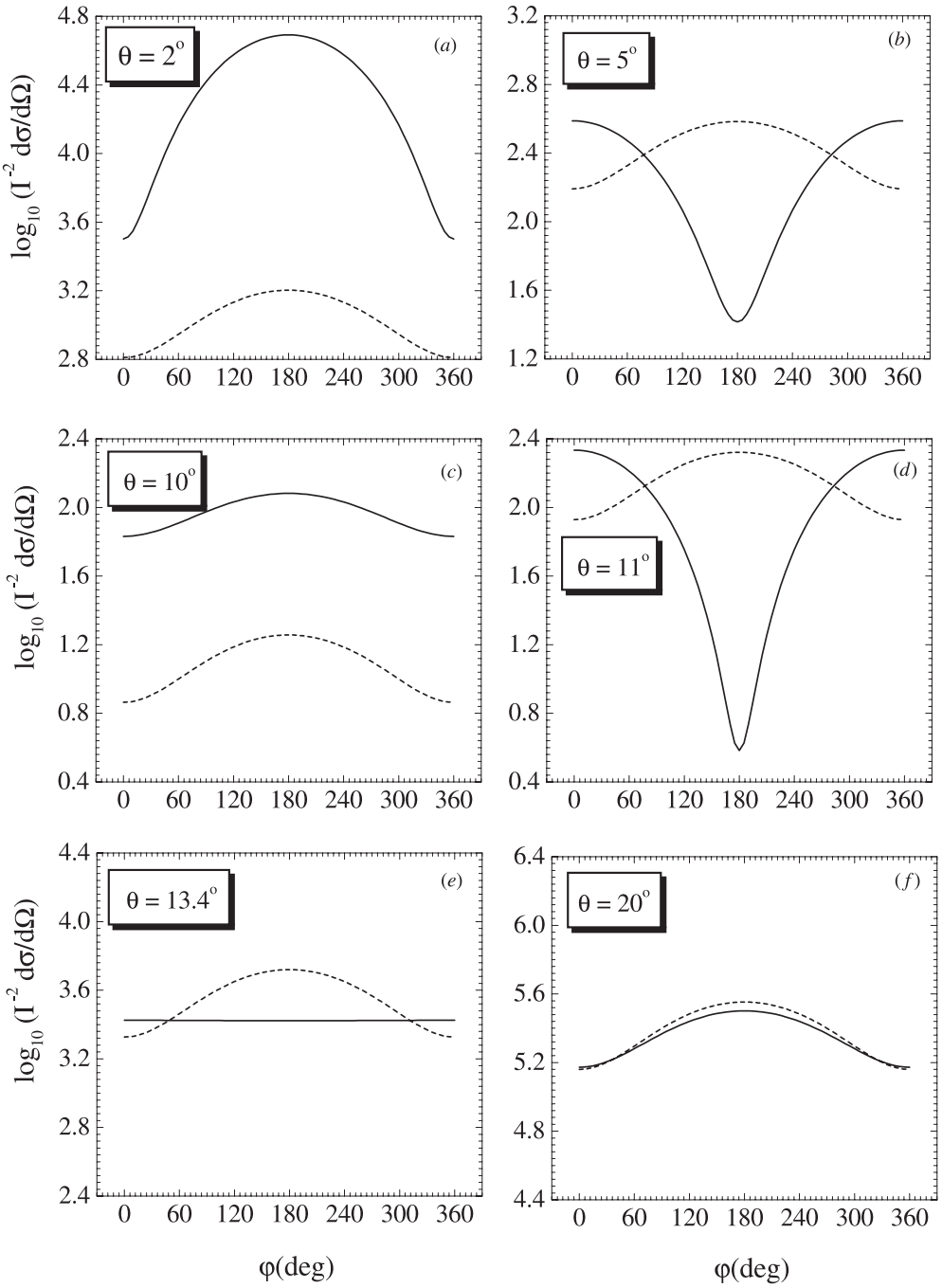

Figure 3. Presents by full curves on a logarithmic scale $I^{-2}\,\mathrm{d}\sigma(+2)/\mathrm{d}\Omega$, evaluated from (16), as a function of the relative phase φ for six values of the scattering angle θ. The dotted curves refer to the same quantity when the target dressing is neglected. The other parameters are the same as in figure 2.

expression for T_b. Of course, this approximation is then a generalization of the Bunkin–Fedorov formula [7] for a bichromatic field. Such calculations were carried out by Varró and Ehlotzky [4–6] in an entirely different regime of parameters, namely $E_i = 10$ eV, $\omega = 0.117$ eV, $I = 4 \times 10^7$ W cm^{-2} and a large scattering angle $\theta = 155^\circ$ in accordance with the experimental work of Weingartshofer *et al* [20]. In this regime the Kroll–Watson low-frequency approximation [8], generalized by Milošević [9] for a bichromatic field, is certainly applicable and at the large scattering angles considered laser dressing of the atom is a negligible effect. Therefore, no specific comparison can be made here with the results of that work.

If the dressing of the target is neglected, the θ dependence of (16) can be written as a prefactor and we obtain

$$\frac{1}{I^2}\frac{\mathrm{d}\sigma(\pm 2)}{\mathrm{d}\Omega} \sim \left[f_{\mathrm{el}}^{\mathrm{B1}}(q)\right]^2 \frac{|(\vec{\varepsilon}\cdot\vec{q})|^4}{\omega^4}\left[1 + \frac{4}{81}\frac{I'}{I} - \frac{4}{9}\sqrt{\frac{I'}{I}}\cos\varphi\right] \tag{19}$$

where $\vec{q}$ is the momentum transfer of the scattered electron and $f_{\mathrm{el}}^{\mathrm{B1}} = 2(q^2+8)(q^2+4^2)^{-2}$ is the transition amplitude in the first-order Born approximation for the elastic scattering by the potential V. Since for $\theta = \arccos(p_i/p_f)$ the scalar product $\vec{\varepsilon}\cdot\vec{q}$ vanishes, the differential cross section (19) also vanishes. At larger scattering angles, where the target dressing no longer contributes significantly, the full and the dotted curves are becoming closer and closer, as we can see for $\theta \geqslant 20^\circ$.

Another important parameter that influences the quantum interference between the two paths in figure 1 is the ratio between the intensities of the two radiation field components, as is apparent in (16). If the dressing is neglected and $I = I'$ then, according to the data in figure 3, the laser-assisted signals (dotted curves) are always increased if $\varphi \neq 0$. For other ratios I'/I the φ dependence can become more complicated. In figure 4 we present $\mathrm{d}\sigma(+2)/\mathrm{d}\Omega$, normalized with respect to I^2, as a function of the scattering angle θ for four different values of the relative phase, namely $\varphi = 0, \pi/4, \pi/2$ and π. In each part we show three curves, evaluated for the following intensity ratios $I'/I = 1$, 10^{-1} and 10^{-2}. If $\varphi = 0$ and if this ratio becomes decreasingly small, then the differential cross sections are correspondingly approaching those cross sections that are determined by path (*a*) of figure 1. In particular, for $I'/I = 10^{-2}$ the three zeros of T_a, discussed previously, can be found at the locations mentioned before. On the other hand, with increasing intensity of the harmonic field, we should recover the differential cross sections originating in path (*b*).

In order to demonstrate the increasing importance of the laser dressing of the atomic target, we show in figures 5 and 6 the cross section data for two-photon absorption ($N = 2$) for the laser frequencies $\omega = 3$ and 4 eV, respectively. The upper frames (*a*) refer to the intensities $I' = I$ and the lower frames (*b*) to $I' = 0.01I$. Evidently, the strong minima, having their origin in a partial cancellation of the two terms $\mathcal{L}(\theta)$ and $\mathcal{L}'(\theta)$ in (17), have now moved, if compared with the data of figure 2, to one or several (larger) scattering angles, in particular in (*b*). These minima can appear at several values of the relative phase φ (0, π, and 2π), indicating the strength of the interference between the matrix elements $\mathcal{T}_a$ and $\mathcal{T}_b$. Hence, with increased laser frequency (and independent of the laser intensity) the angular distribution of the scattered electrons becomes richer in its details, to a large extent due to the stronger influence of the laser field and of its harmonic on the structure of the atomic states. Therefore, coherent phase control is also becoming of increased interest at higher radiation frequencies.

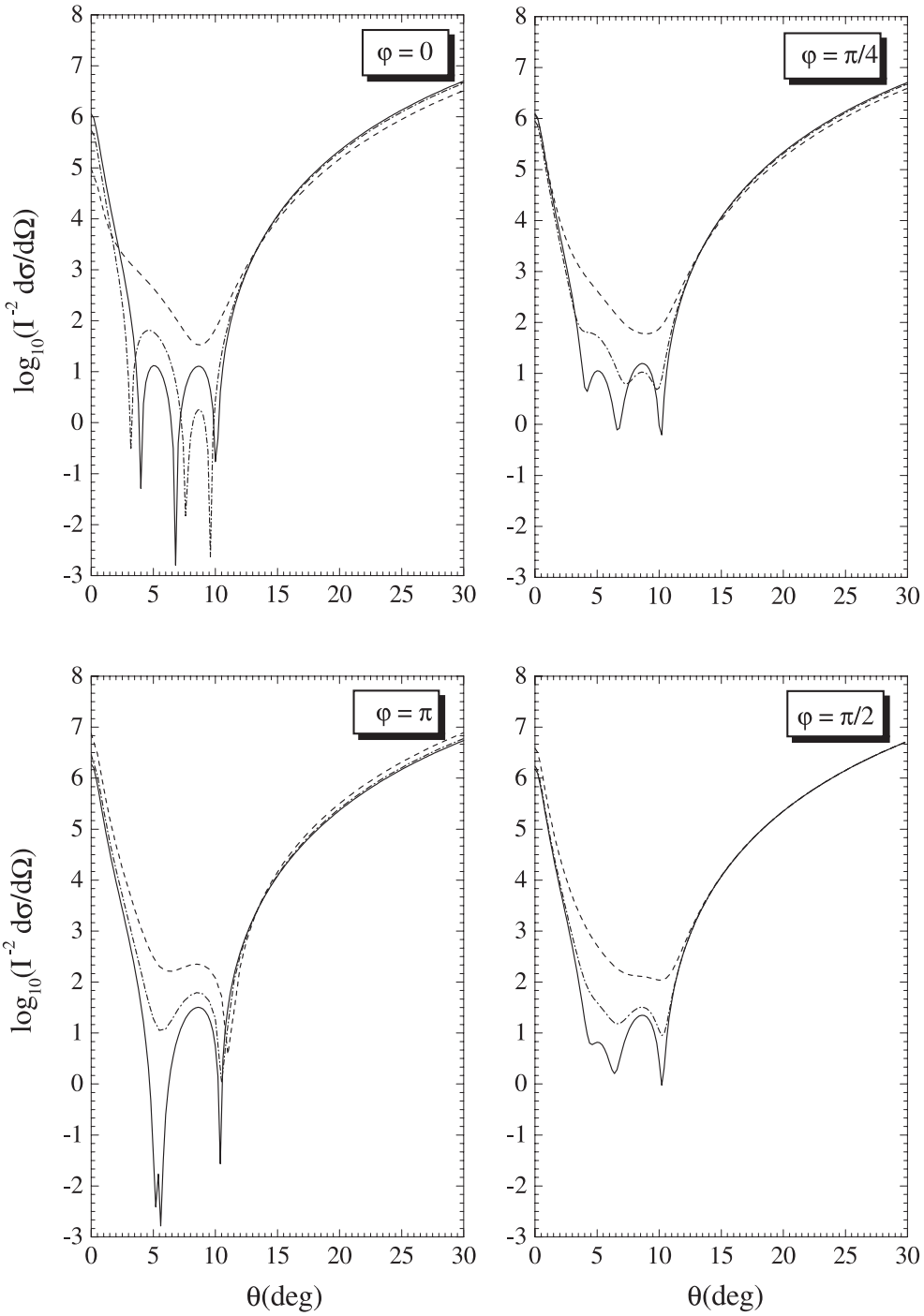

Figure 4. $I^{-2}\,\mathrm{d}\sigma(+2)/\mathrm{d}\Omega$ is shown on a logarithmic scale as a function of the scattering angle θ for four values of the relative phase: $\varphi = 0$, $\pi/4$, $\pi/2$ and π. The initial electron energy and the laser frequency are the same as before. The intensity of the harmonic field is 1% of the laser intensity (full curves), 10% (chain curves) and 100% (broken curves).

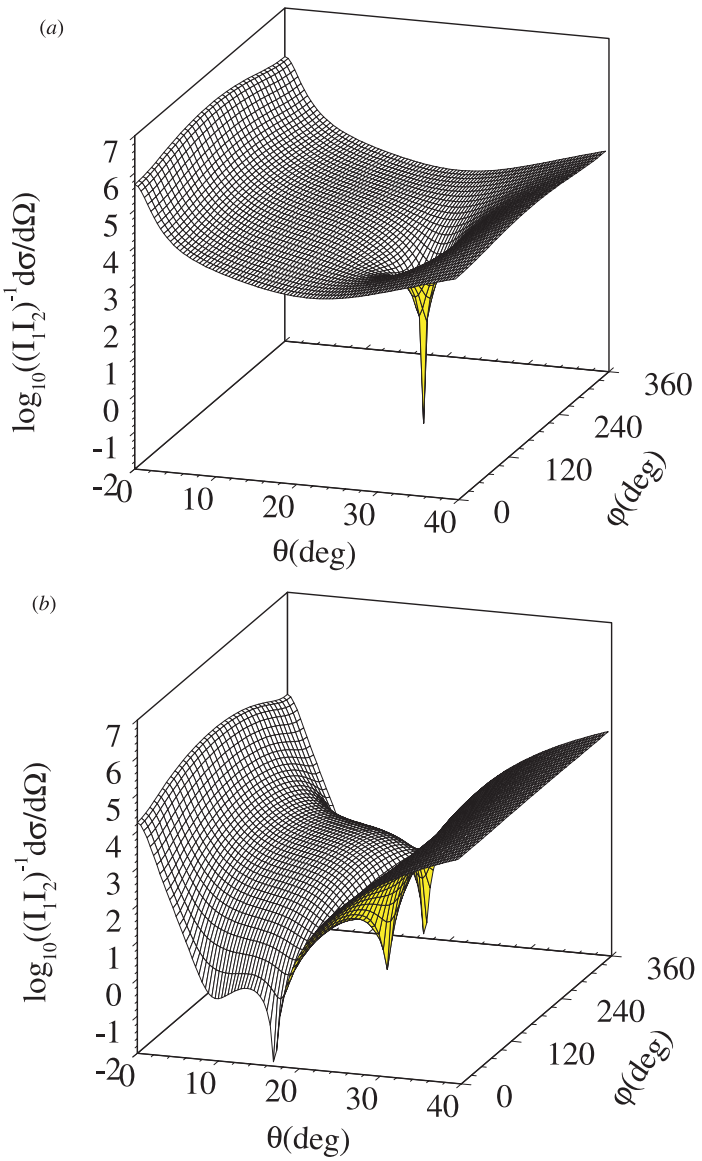

Figure 5. Cross section data for $N = 2$ as a function of θ and φ for the laser frequency $\omega = 3$ eV and its third harmonic. In (*a*) $I' = I$ and in (*b*) $I' = 0.01I$. The dependence of the data on the ratio of the intensities is remarkable as well as increasing the richness of the angular distribution with increased laser frequency, if compared with the data of figure 2.

4. Summary and conclusion

In this paper we have studied the effect of the relative phase between the harmonic field of frequency 3ω and the fundamental field of frequency ω on two-photon free–free transitions in laser-assisted electron–hydrogen scattering. Using third-order perturbation theory and taking into account all the Feynman diagrams involved, we evaluated the differential cross sections for scattered electrons of energy $E_f = E_i \pm 2\omega$. For fast scattered electrons and

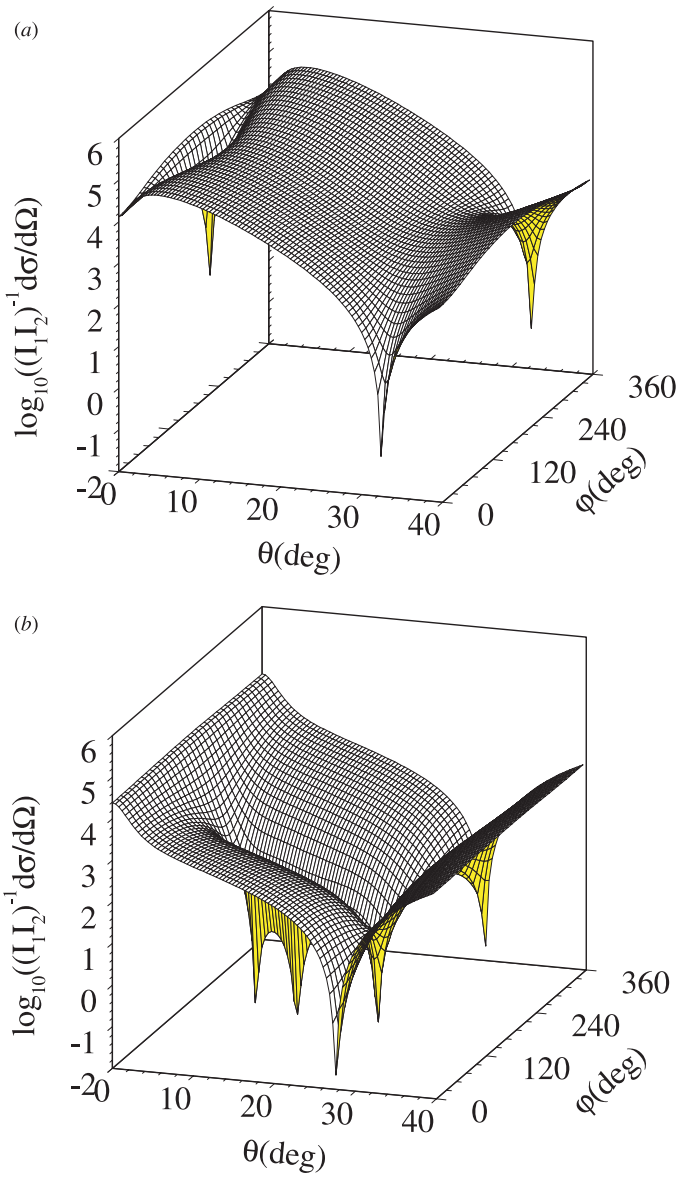

Figure 6. Similar data for $\omega = 4$ eV. The other parameters are the same as in figure 5. A comparison with figure 5 makes clear the strong dependence of the results on the laser frequency.

low field intensities, as well as at smaller scattering angles where the dressing is important, the interference between the two quantum paths leading to the foregoing final energies are modulated by changing the relative phase φ. The signature of the target dressing by the bichromatic field was discussed for fast electrons and low radiation field intensities in the region of smaller scattering angles, where the dressing effects are important. We concluded that whenever the target dressing cannot be neglected, it significantly influences the phase dependence and the effect of the radiation field on the atomic states is increasing with increasing laser frequency ω.

Acknowledgments

This work was supported by a special research project for 2000/1 of the Austrian Ministry of Education, Science and Culture. We also acknowledge financial support by the University of Innsbruck under reference number 17011/68-00.

References

[1] Shapiro M, Hepburn J W and Brumer P 1988 *Chem. Phys. Lett.* **149** 451
[2] Shapiro M and Brumer P 2000 *Adv. At. Mol. Opt. Phys.* **42** 287
[3] Ehlotzky F 2001 *Phys. Rep.* **345** 175
[4] Varró S and Ehlotzky F 1993 *Phys. Rev.* A **47** 715
[5] Varró S and Ehlotzky F 1993 *Opt. Commun.* **99** 177
[6] Varró S and Ehlotzky F 1995 *J. Phys. B: At. Mol. Opt. Phys.* **28** 1613
[7] Bunkin F V and Fedorov M V 1965 *Zh. Exp. Teor. Fiz.***49** 1215 (Engl. transl. 1966 *Sov. Phys.–JETP* **22** 844)
[8] Kroll N M and Watson K M 1973 *Phys. Rev.* A **8** 804
[9] Milošević D B 1996 *J. Phys. B: At. Mol. Opt. Phys.* **29** 875
[10] Rabadán I, Méndez L and Dickinson A S 1996 *J. Phys. B: At. Mol. Opt. Phys.* **29** 163
[11] Lami A and Rahman N K 1981 *J. Phys. B: At. Mol. Phys.* **14** L523
[12] Lami A and Rahman N K 1983 *J. Phys. B: At. Mol. Phys.* **16** L201
[13] Varró S and Ehlotzky F 1997 *J. Phys. B: At. Mol. Opt. Phys.* **30** 1061
[14] Ghalim M and Mastour F 1999 *J. Phys. B: At. Mol. Opt. Phys.* **32** 3794
[15] Dubois A, Maquet A and Jetzke S 1986 *Phys. Rev.* A **34** 1888
[16] Kracke G, Briggs J S, Dubois A, Maquet A and Véniard V 1994 *J. Phys. B: At. Mol. Opt. Phys.* **27** 3241
[17] Cionga A and Buică G 1998 *Laser Phys.* **8** 164
[18] Cionga A and Zloh G 1999 *Laser Phys.* **9** 69
[19] Cionga A and Florescu V 1992 *Phys. Rev.* A **45** 5282
[20] Weingartshofer A, Holmes J K, Sabbagh J and Chin S L 1983 *J. Phys. B: At. Mol. Phys.* **16** 1805